3. Experimental setup and methodology

3.1 Experimental setup

In order to investigate the scour hole evolution downstream of a rigid bed, a series of experimental runs have been carried out in a straight channel realized at the laboratory of Department of Hydraulic Engineering and Environmental Applications, University of Palermo. A photo of the experimental apparatus is reported in Figure 3.1.

Figure 3.1 – Photo of the experimental apparatus.

The experimental runs have been carried out in a rectangular flume 12 m long and 0.4 m wide. In the first reach of the channel (3.5 m long) the bed was rigid and in the remaining part (8.5 m long) the bed was mobile. In Figure 3.2, a plane view of the experimental apparatus is reported. The channel reach characterized by rigid bed allows to gradually reduce the energy of the water flow coming from the recirculating pumping system. Within this first rigid-bed reach a series of horizontal and vertical wood and PVC pipes, have been arranged in order to dissipate the excessive energy of the incoming flow

and to uniformly spread the flow over the initial cross section (see plots reported in Figure 3.3). The channel walls of this channel reach is realized with thin sheets of Plexiglas strips. The bed (slope i = 0.1%) was rigid and realized with a panel of wood covered by the same sand as the mobile channel reach. Downstream of such rigid bed reach the bed of the channel is deformable.

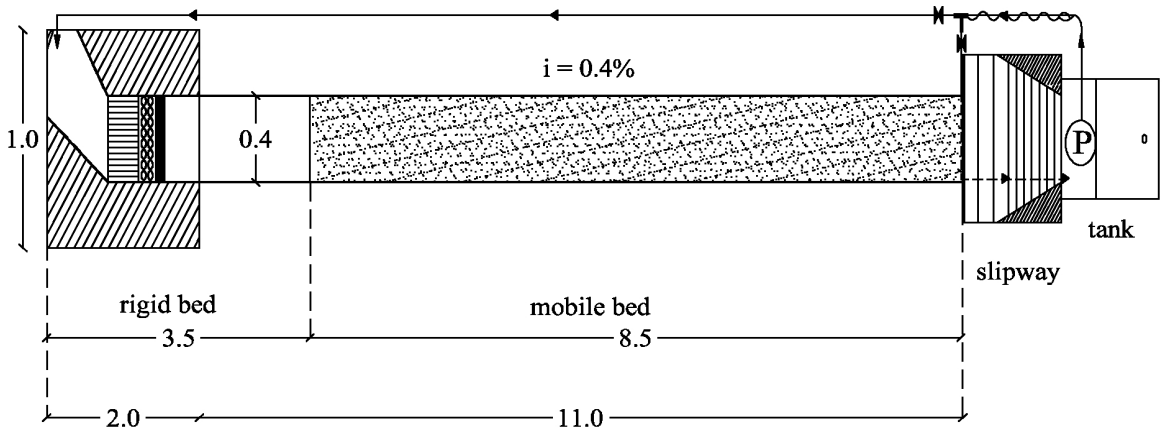

Figure 3.2 – Plane view of the experimental apparatus.

Figure 3.3 – Two photos of the inlet channel reach.

The walls of the mobile-bed channel reach are made of Plexiglas strips with a thickness of 1cm. The bed is of quartz sand with a specific gravity of 2.65 (D_{50} = 0.86 mm

and σ_g = 1.27). A mobile gate, at the downstream end of the mobile-bed reach, is used to adjust the water-depth (see planeview in Figure 3.2).

The recirculating system consists of a pipeline (PVC, ϕ = 100 mm, nominal pressure of PN16) and a centrifugal pump (ABS-JUMBO - 50Hz with a maximum output power of 5.8kW) plunged into the downstream tank (Figure 3.2). The water is supplied to the inlet channel by the pump, passing through the regulating valves (see Figure 3.2).

The pump system allows us to recirculate a water discharge of about 35 l/s, with hydraulic head of 1.2 m. The downstream tank is divided into two parts separated by grid that allows to deliver both water and sand to the channel. The pump is placed in the first part of the tank upstream of such grid.

– *Sediment characteristics and incipient motion*

The grain size distribution of the sand used for the experiments has been determined by an automatic sifter, VibroMaster200, shown in Figure 3.4a. The grain size distribution obtained, reported in Figure 3.4b, is on a semi-logarithmic plane, being D_x the diameter of sand corresponding to x % passing in weight, $P(\%)$. The value of D_{16}, D_{50} and D_{84} of the sand are reported in table 3.1. The geometric standard deviation, which allows to describe the sand distribution is:

$$\sigma_g = \sqrt{\frac{D_{84}}{D_{16}}} = 1.27 \qquad (3.1)$$

Thus, the sand can be classified as well-sorted ($\sigma_g \leq 1.3$).

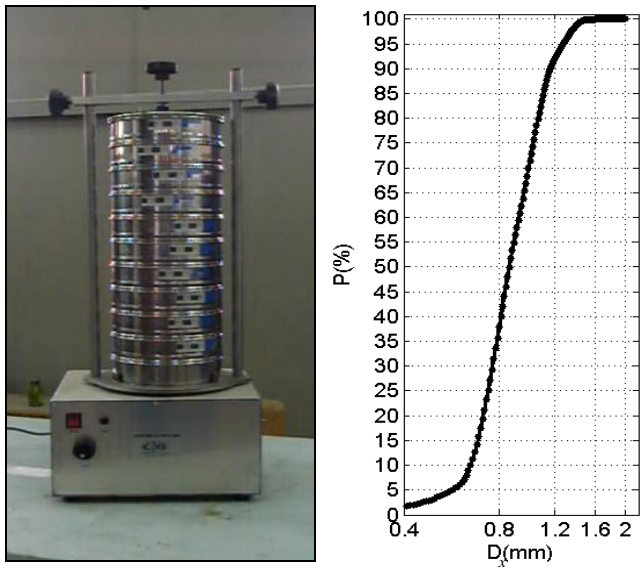

a) b)

Figura 3.4 – a) Sifter - VibroMaster 200; b) grain size distribution.

Estimation of particle sizes

Sand Diameter	***Value***
D_{16}	0.68
D_{50}	0.865
D_{85}	1.099

Table 3.1. The geometric characteristics of the sand used for the experiments.

In order to evaluate the bed slope the *Critical Shields Number* θ^* by using the expression proposed by Guo (1990):

$$\begin{cases} \theta^* = \dfrac{0.1}{\mathrm{R}_*^{2/3}} + 0.054 \cdot \left[1 - exp\left(-\dfrac{\mathrm{R}_*^{0.52}}{10} \right) \right] \\ \mathrm{R}_* = \dfrac{D_{50}\sqrt{0.1 \cdot (s-1) \cdot g \cdot D_{50}}}{\upsilon} \end{cases}; \qquad (3.2)$$

where R_* is the Rouse Reynolds number, s is the specific gravity of sediment ($s = \rho_s / \rho_w$, ρ_w water density and ρ_s sand density).

Thus, the critic shear stress, τ_c, has been estimated as:

$$\tau_C = \theta^* (s-1) \cdot \gamma \cdot D_{50} \tag{3.3}$$

where $\gamma$is the specific weight of water.

The critical slope i_c has been determined as:

$$i_c = \frac{\gamma \cdot \Re}{\tau_c} \tag{3.4}$$

with $\Re$ the hydraulic radius

A summary of the estimated parameters is reported in table 3.2. Finally the longitudinal bed slope of the mobile-bed channel reach has been assumed equal to 0.4%.

Estimated Parameters	***value***
Submerged specific gravity of bed particles : (*s*-1)	1.65
*Rouse parameter – R**	1.20
*Critic Shields Number – θ**	0.094
Critic shear stress – τ_c[N/m^2]	1.3
Critic slope : i_c	0.002

Table 3.2. Estimation of the critical parameters.

3.2 Experimental runs

In order to obtain the scour hole downstream of the rigid-bed reach two different runs have been carried out. First, a mobile-bed run, has been performed in order to measure the temporal evolution of the bed surface downstream of the rigid-bed until the reaching of the "equilibrium" configuration. Then a second run, over the final deformed bed configuration, has been conducted in order to measure the flow velocity field into the scour hole developed downstream of the rigid bed. These runs were conducted under

steady flow conditions with a water discharge of Q = 35 l/s. The hydraulic parameters considered for each run are reported in Table 3.3.

Hydraulic Parameters	h_0**(cm)**	U_0**(m/s)**	U_k**(m/s)**	***Fr***	***Re***	***Re****	u^***(m/s)**
values	9.3	0.98	0.95	1.04	$4 \cdot 10^5$	45	0.05

Table 3.3. Hydraulic Parameters during both runs.

where *ho* is the water depth over the rigid bed, U_0 is the average velocity of the flow, U_k is the critical velocity of the flow, *Fr* is the Froude number, *Re* the Reynolds number and u^* is the shear velocity.

During both runs the water discharge was monitored through the ultrasonic area-velocity Meanstream EH7000.

The origin of the reference system used for measurements is the right bank of the first section of the mobile bed channel reach (initial section X0), as reported in Figure 3.5. The longitudinal axis X has positive versus according the flow direction and the transversal axis Y is horizontal has positive versus towards the right bank (see Figure 3.5a). The vertical axis, Z, has positive versus toward the free surface (see Figure 3.5b). Thus, the horizontal plane including the initial section has been assumed as reference plane.

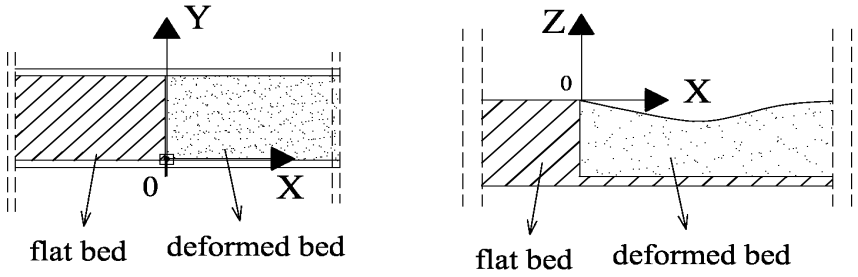

a) b)

Figure 3.5 - Reference system along longitudinal X, transversal Y and vertical direction Z: a) plan view; b) longitudinal view.

The mobile-bed run started with no sediment upstream supply, so that scouring process developed in clear-water condition (see paragraph 2.1). During the experiment, both water and sediment were recirculated through the pumping system described in paragraph 3.1. The duration of the run was about of T = 480 min, at which the "equilibrium" configuration was reached. In this work the “equilibrium” condition was considered as the time when the scour depth did not change significantly. It was observed that during the run both the depth and the length of the scour hole oscillated around an equilibrium condition, in agreement with Richardson and Davis (2001). Moreover, in order to verify the reaching of the “equilibrium” condition, the sediment discharge has been monitored at regular time intervals (ΔT = 30÷60 min) by using a movable sediment trap. The sediment trap (here called MPS09), located at the end of the channel into the slipway, is a wooden box with a metal grid at the bottom. A photo of the MPS09 tool is reported in Figure 3.6a. In Figure 3.6b the sediment discharge is plotted against time. The plot shows that for times t < 1 h the water discharge quickly increases; for t = 1 ÷ 2 h q_s increases slowly; at t = 2.5 h, q_s reaches a peak value of 35g/s and finally for $t \geq 4$ h, q_s maintains.

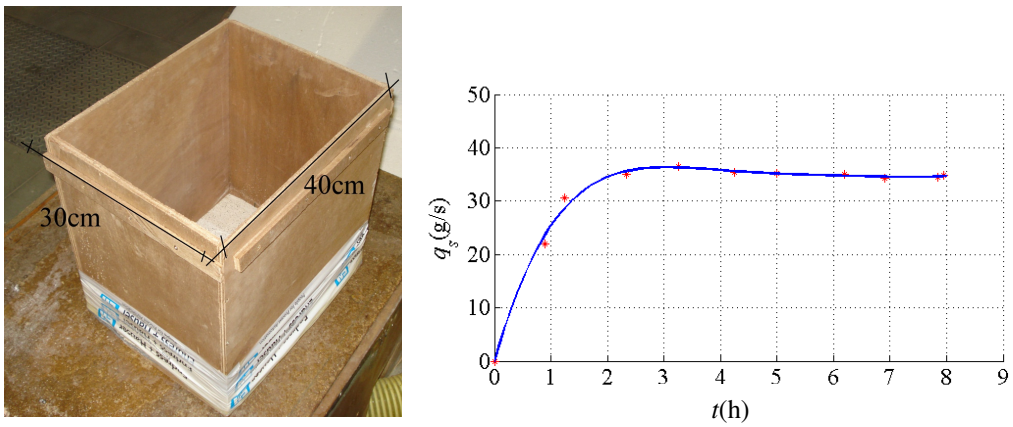

a) b)

Figure 3.6 – Sediment discharge: a) sediment trap MPS09; b) plot of q_s - t.

The evolution of the bed was measured by using a profile indicator by Delft Hydraulics (with precision of 0.1 mm). The instantaneous bed levels were acquired along the transversal direction in measurement sections selected along the mobile-bed reach, 7.5m long. In Figure 3.7 is reported a scheme of the measurement sections. The measurement channel reach was divided into three parts of equal length so that the mutual distance, ΔX, between the measurement sections included in each part was assumed greater as the distance of the stretch from the initial section (initial section = first section of the mobile-bed channel) increased. In particular, it was assumed ΔX = 5 cm in the first stretch (stretch nearest to the initial section), ΔX = 10 cm in the second stretch and ΔX = 15 cm in the third stretch.

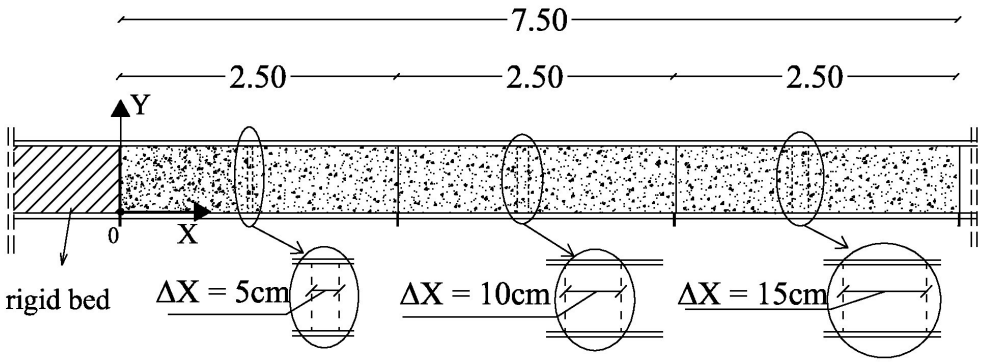

Figure 3.7 – Measurement sections for the instantaneous bed level investigation.

Finally, 92 measurement sections were considered. Hereon, each cross section is called with notation Xj (with j = 0,…,750) where j indicates the corresponding longitudinal distance (in cm) from the initial section. For each measurement section the instantaneous bed profiles were acquired; the first and the last measurement point of each transversal profile were 4 cm distant from each bank. Thus each bed profile was measured for Y = 4 ÷ 36cm, with a transversal step dY = 1cm. The bed profiles in each section were

measured at time intervals of 20÷30 min. Thus 25 instantaneous configurations of the deformed bed were obtained.

At the end of the mobile-bed run the final bed surface was stiffened by using a cement dust. In Figure 3.8 a photo of the lateral view of the final scour hole (first 50cm downstream the rigid bed) is reported.

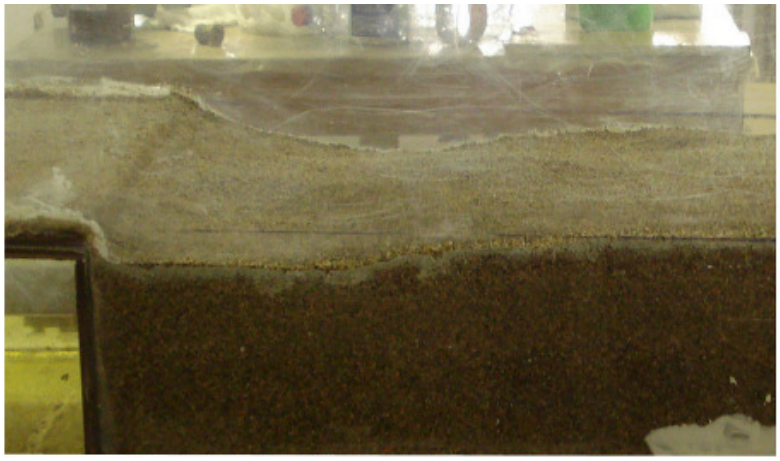

Figure 3.8 – Equilibrium scour hole.

Then the rigid-deformed-bed run was carried out. In order to analyze the flow velocity field in the scour hole, the instantaneous longitudinal, $u_x(t)$, transversal, $u_y(t)$, and vertical, $u_z(t)$, velocity components were measured along the channel reach (50 cm long) interested by scouring phenomenon (see Figure 3.8). For measurements the positive versus of the velocity components was assumed in agreement with the positive versus of the reference system.

The longitudinal and vertical velocity components were measured using a two-dimensional laser anemometer – LDA2D by Dantec s.r.l.; the transversal velocity component was measured using an ultrasonic anemometer DOP2000 by Signal Processing s.a. The measurement points were selected in the considered measurement sections so that

their mutual distance was, in each cross section, of dZ = 0.3 cm along the vertical direction Z and along the transverse direction Y the measurement step was of dY = 1 cm.

3.3 Measurement Instruments

As aforementioned Profile Indicator - PV09 by Delft Hydraulics was used to measure the evolution of the bed level during mobile-bed run. A Laser Doppler Anemometer (LDA2D) was employed to measure the longitudinal and vertical velocity components ($u_x(t)$ and $u_z(t)$, respectively) and the ultrasonic velocimeter DOP2000 was used to acquire the transversal component ($u_y(t)$).

3.3.1 Profile Indicator – PV09

The Profile Indicator (PV09) is designed to maintain a constant distance between the probe and the bed (or between the probe and the free surface) in order to maintain a constant electric capacity. Thus, the instrument is able to monitor the temporal or the spatial variation of the bed (or the free surface). The profile indicator was used during the mobile-bed run to measure the instantaneous bed level data at each measurement section, as it has been described in paragraph 3.2. It measured the bed elevation with a sampling frequency of 100 Hz with a sensitivity of 0.2 mm and a precision of 0.1 mm.

The instrument is made of a gauge with a probe, a remote control (RCU) and a PC card NI-DAQ (see Figure 3.9). The probe is continuously positioned at a fixed, but adjustable distance of 0.5 to 2 mm (bed material dependent) over the bed level by a servo-controlled bridge balance circuit. A vertical position transducer, coupled to the servo output-shaft gives an analogue output signal (Figure 3.9b).

The probe is a stainless tube insulated by a cover (see Figure 3.10) and it is fitted in the gauge (Figure 3.9b).

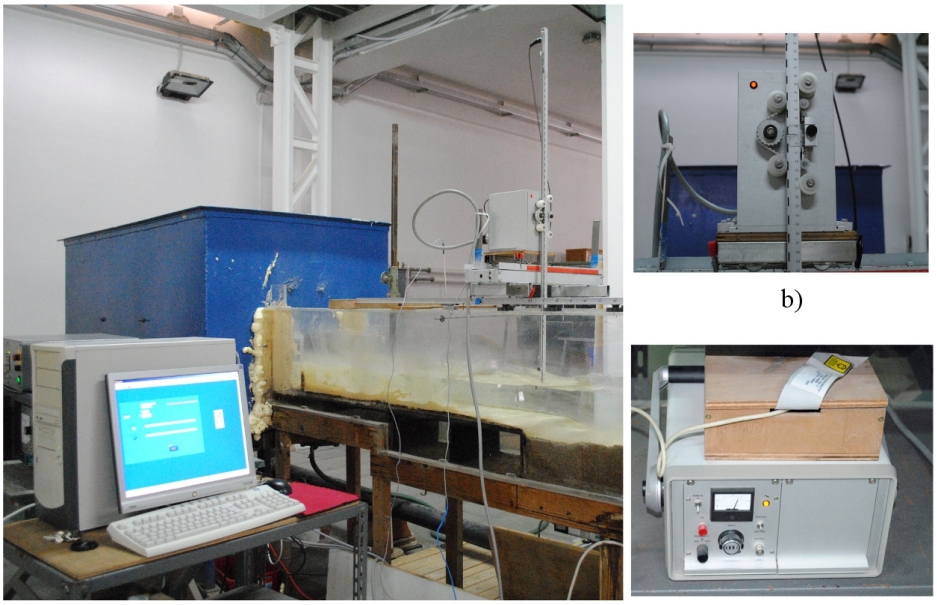

a) b) c)

Figure 3.9 – Some details of the Profile Indicator - PV09: a) photo of the whole system; b) gauge; c) RCU;

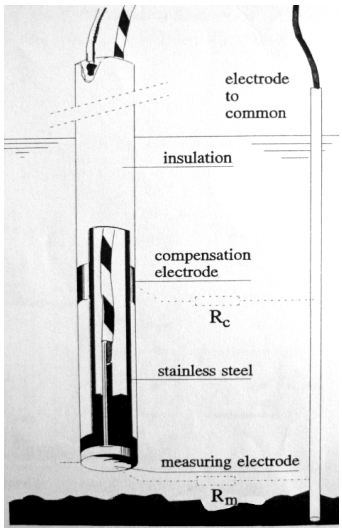

Figure 3.10 – Probe tip.

A stainless-steel ring interrupts the insulation at 24 mm from the probe and forms the so called compensation electrode while the tip is the measuring electrode (see Figure 3.10). When the gauge is placed into a fluid, a common electrode have to be placed

somewhere at the bottom. With respect of the common electrode both the compensation and the measuring electrode form a resistor in the fluid: the resistors *Rm* and *Rc* being part of a Wheatstone bridge.

The full instrument control is incorporated in the local transmitter (Figure 3.9b). Moreover a Remote Control Unit (RCU) provides full control of all transmitter functions and the required power supply (see Figure 3.9c).

The analogical output is converted into digital, filtered and recorded through a PC card NI-DAQ - PCI 6024E by National Instruments and a data acquisition algorithm compiled in Labview (ver. 9.0) environment.

3.3.2 Laser Doppler Anemometer – LDA2D

The LDA2D (Flowlite2D, by Dantec) is an optical system able to acquire two velocity components in a completely non-intrusive way. The principle of operation of the instrument is based on the Doppler effect. The Dantec system consists on a laser source (Argon-ion 300 mW), the transmitting optics (beam splitter and Bragg cell with a frequency shift (f_{shift}) of 40 MHz), receiving optics, a Burst Spectrum Analyzer (BSA F60 processor) and a traversing system. Figure 3.11 reports some details of LDA2D system.

The laser beam is splitted by a Bragg cell (see Figure 3.11c) in two laser beams of equal intensity with frequencies f_0 and f_{shift}. These are focused in optical fibres bringing them to a probe (Figure 3.11b). A Bragg cell is a glass crystal with a vibrating piezo crystal attached. The vibration generates acoustical waves acting like an optical grid. In the probe, the parallel exit beams from the fibers are focused by a lens to intersect in the probe volume. Moreover, the LDA2D system has a color splitter that divides each laser beam in two laser beams with different color and length wave. In Figure 3.12 is reported a scheme of the LDA2D optical system. Therefore the laser optic emits two couples of laser

beam of two different colors: a blue laser beam with λ = 514.4 nm and a green laser beam of λ = 488 nm.

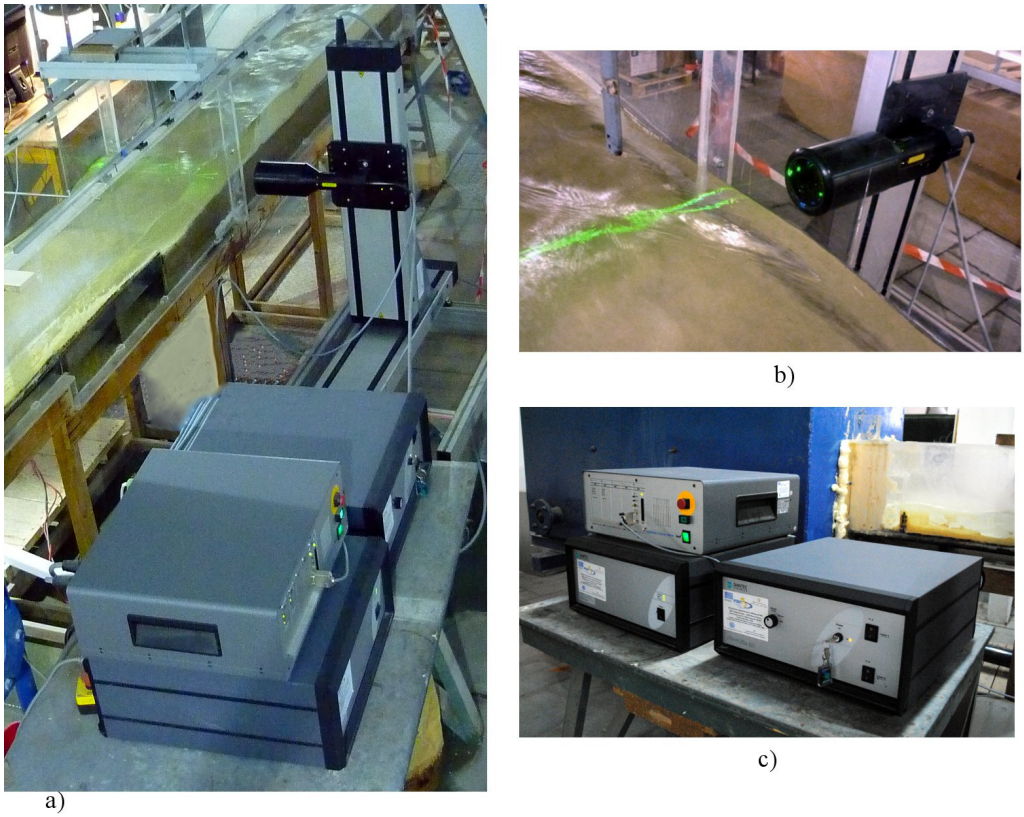

Figure 3.11 – Some details of the LDA2D System: a) photo of Flowlite2D; b) transmitting optic system; c) FlowLite and BSAF60.

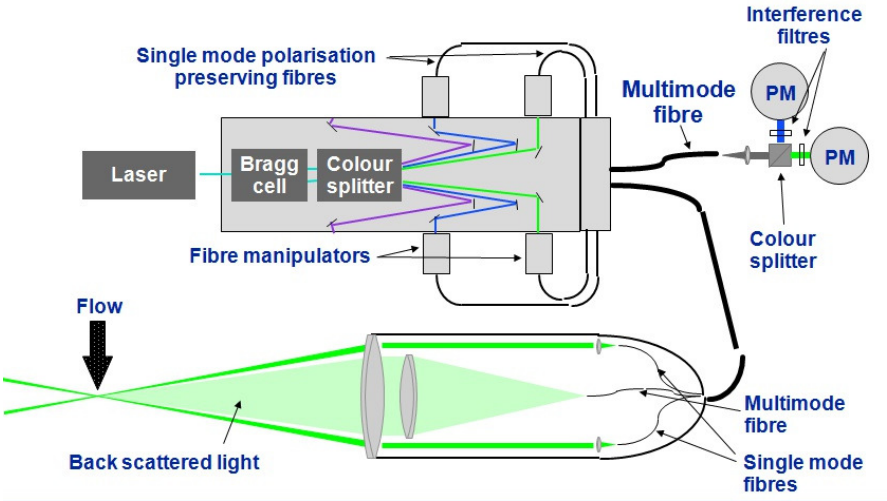

Figure 3.12 – Scheme of the transmitting and receiving optics – Flowlite2D.

The LDA2D acquires two velocity components: the longitudinal component $u_x(t)$ is measured by the green laser beam couples and the vertical velocity component $u_z(t)$ is measured by the blue laser beam couples. The sampling volume is typically a few millimeters long and it has a shape of a lengthen ellipsoid. The dimension of the probe volume depends on the wave length of the laser beam.

The light intensity is modulated due to interference between the laser beams. This produces parallel planes of high light intensity, so called fringes. The fringe distance d_f is defined by the wavelength λ of the laser light and the angle θ between the couple of beams:

$$d_f = \frac{\lambda}{2\,sin(\theta/2)} \tag{3.5}$$

When the particle crosses this fringe pattern, the scattered light fluctuates in intensity with a frequency equal to the velocity v of the particle divided by the fringe spacing d_f. Thus, the velocity of that particle is:

$$v = d_f \cdot f_D = \frac{\lambda}{2\,sin(\theta/2)} \cdot f_D \tag{3.6}$$

where f_D is the frequency (Doppler frequency) of the light scattered by the tiny "seeding" particles carried in the fluid moving through the probe volume. The velocity v is the velocity component perpendicular to the bisector of the two laser beams.

The back scattered light is collected by a receiver lens and focused on a photo-detector (see Figure 3.12). An interference filter, mounted before the photo-detector, passes only the required wavelength to the photo-detector. This removes noise from ambient light and from other wavelengths.

The photo-detector converts the fluctuating light intensity to an electrical signal, the Doppler burst, which is sinusoidal with a Gaussian envelope due to the intensity profile of the laser beams. The Doppler bursts are filtered and amplified in the signal processor

(BSA processor), which determines f_D for each particle. The BSA processor uses the Fast Fourier Transform (FFT) principles and a multi-bit signal quantization to improve performance (accuracy of about 1%), with regards to turbulent flow measurement, and handling of noisy signals.

By observing equation 3.4 it is clear that without the shift frequency (f_{shift} = 40 MHz) the LDA system could not distinguish between positive and negative flow direction or measures null velocity. Thus the f_{shift} is used by the BSA processor to remove the directional ambiguity.

The LDA system measure the velocity of particles suspended on the flow. The rigid-deformed-bed run has been conducted in clear-water condition, thus the water flow has been seeded. The seeding particles used during the run were of marble dust. This seeding particles were small enough to follow the flow (the range of particles were between 10 µm and 100 µm), yet large enough to scatter sufficient light to obtain a good signal-to-noise ratio at the photo-detector output.

The duration of velocity acquisition is strictly dependent on the sampling frequency and on the number of samples. The sampling frequency is not constant during the acquisition because the velocity range and the density of seeding particles could change. Thus in order to choose the right temporal acquisition a preliminary run has been conducted. During this test some velocity samples have been acquired in points located near the bed and close to the free surface. The time series have been analyzed in order to observe at what time T the mean value of the velocity components continue to be constant. In Figure 3.13 are reported the time-average series of the velocity longitudinal and vertical components. The time-averaged values of the longitudinal component $U_x(t)$ maintain a constant value for T = 30 ÷ 40 sec (10000 ÷ 15000 samples). The time-averaged values of the vertical component $U_z(t)$ are constant for T = 40 ÷ 50 sec (5000 ÷ 10000 samples).

Thus, for each measuring point the following two criteria have been considered: for the longitudinal component 15000 samples (minimum 40 sec sampling time) and for the vertical component 10000 samples (minimum 50 sec sampling time).

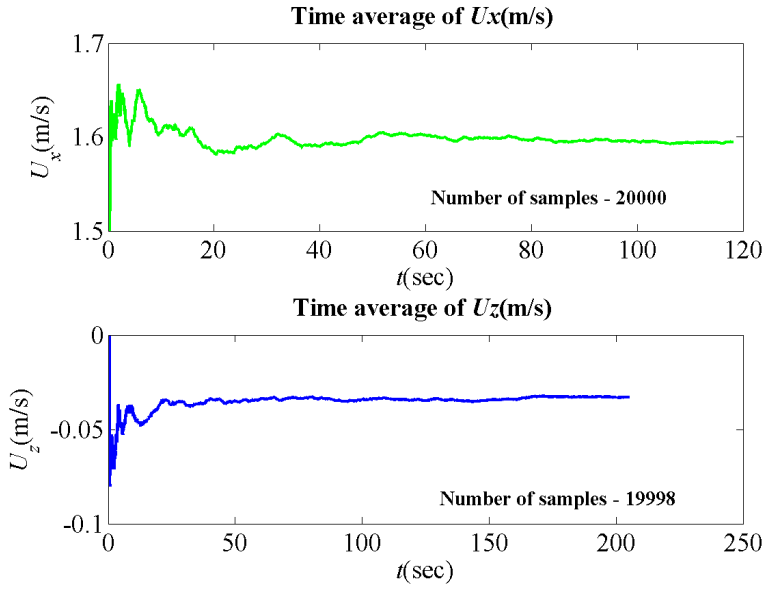

Figure 3.13 - Time-average values of the longitudinal $U_x(t)$ and vertical $U_z(t)$ components.

3.3.3 Ultrasonic Velocimeter – DOP2000

The DOP2000 (by Signal Processing) is an ultrasonic anemometer that measures the instantaneous velocity profile along direction of the probe axis (see Figure 3.14a). The ultrasonic anemometer operates through its embedded computer and a series of probes (Figure 3.14b). The computer enables manage settings of the probes and displays in real time the velocity samples acquired by the probes. This anemometer is a pulsed Doppler ultrasound, thus the velocities are derived from shifts in positions between pulses. In pulsed Doppler ultrasound, instead of emitting continuous ultrasonic waves, an emitter sends periodically a short ultrasonic burst and a receiver collects continuously echoes reflected from targets that may be present in the path of the ultrasonic beam.

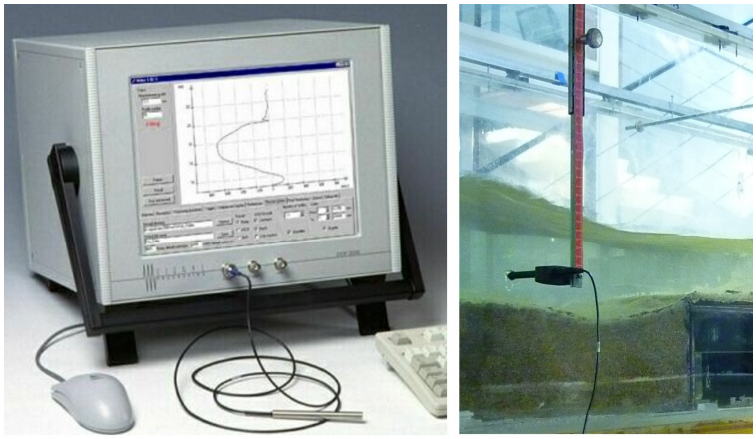

a) b)

Figure 3.14 – a) DOP2000; b) the 8MHz probe orthogonal to a channel wall.

By sampling the incoming echoes at the same time relative to the emission of the bursts, the shift of positions of scatters are measured. The velocity of a suspended particle invested by an ultrasonic beam is expressed as:

$$v = \frac{c}{2 \cdot f_e \cos(\theta)} \cdot f_D \tag{3.7}$$

where f_D is the doppler frequency, f_e is the emitted frequency, θ is the angle between the velocity vector and the emitting axis and c is the velocity of sound in water.

An important parameter of this velocimeter is the pulse repetition frequency PRF that is the ultrasonic burst frequency. At each value of PRF corresponds a maximum velocity v_{max} measured:

$$v_{max} = \frac{c}{2 \cdot f_e \cos(\theta)} \cdot \mathrm{PRF} \tag{3.8}$$

The pulse repetition frequency also gives the maximum time allowed to the burst to travel to the particle and back to the transducer. This gives a maximum depth d_{max} of:

$$d_{max} = \frac{c}{2 \cdot \mathrm{PRF}} \tag{3.9}$$

The DOP2000 has been used to determine the velocity component along the transversal direction at the same measurement points considered for the LDA acquisition. The velocity data were collected through an ultrasonic probe (by Signal Processing) positioned in transverse direction outside of the channel walls (see Figure 3.14b). Thus the probe was used such as transmitter and receiver. The transducer was a probe with a case 9 mm long, 5 mm diameter and it has with an ultrasonic frequency of 8 Mhz. In order to acquire the whole width of the water flow the pulse repetition frequency was settled to 1000 KHz. The number of the emitted profiles was of 500 and the distance between the centres of adjacent sampling volumes was of about 5 mm. In a previous test these configuration have been tested in order to verify if the acquisition time (120sec) was enough to maintain a constant value of the time-average velocity *Uy*. In Figure 3.15 the time series *Uy*(*t*) relative to a point near the bed and to a point near the free surface are reported. The plots show that the mean value stay constant for T ≥ 60-70sec, thus a time acquisition of 120 sec is enough.

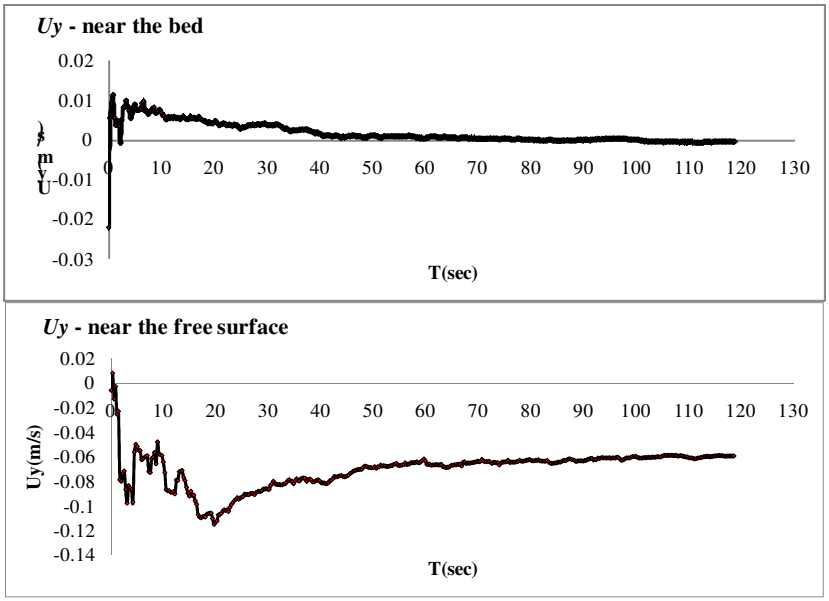

Figure 3.15 – Time-averaged *Uy* for two measurement points.